Application of Intelligent Control in Chromatography Separation Process

Chao-Fan Xie , Hong Zhang , Rey-Chue Hwang *

Posted Date: 7 November 2023

doi: 10.20944/preprints202311.0420.v1

Keywords: Chromatographic separation; SMB; multi-column; fuzzy; neural network

Article

Application of Intelligent Control in Chromatography Separation Process

Chao-Fan Xie [1], Hong Zhang [2] and Rey-Chue Hwang [3,*]

[1] School of Big Data and Artificial Intelligence, Fujian Polytechnic Normal University, Fuqing, 350300, China; 119396356@qq.com

[2] Key Laboratory of Nondestructive Testing, Fujian Ploytechnic Normal University,Fujian Province University, China, zhhgw@hotmail.com

[3] Department of Electrical Engineering, I-Shou University, Kaohsiung, Taiwan; rchwang@isu.edu.tw

* Correspondence: rchwang@isu.edu.tw, Tel.: 886-0928722593

Abstract: Chromatographic separation is a critical technique in the manufacturing processes of both chemical products and biopharmaceuticals. Its principle relies on exploiting the differences in distribution between the stationary and mobile phases to achieve the separation of mixtures. The precision of substance concentration during separation directly impacts the quality and usability of the final product. Therefore, the development of an effective and precise separation control technique has long been a vital concern in the field of chromatographic separation control. Currently, the employment of Simulated Moving Bed (SMB) technology for chromatographic separation, which allows for continuous feed, has been recognized as a cutting-edge technique. SMB is a continuous process technology that enhances the efficiency of adsorbents within the bed. This sequential multi-column SMB technology not only increases production capacity but also reduces the consumption of solvents and water. It is acknowledged as one of the cleanest manufacturing technologies in the biopharmaceutical industry. However, multi-column SMB involves various variables such as flow rates in multiple sections and valve switching times, rendering its system control highly complex. Unlike traditional control objectives that aim to minimize control output errors, the control objective of SMB is to achieve a specific proportion of substance concentration. Consequently, designing and implementing traditional control theories for SMB is challenging, leading to SMB systems largely being controlled based on simple PLC controls. Moreover, these controls are often applicable only to single or a few-column SMB setups, limiting the effectiveness of high-capacity applications. To achieve effective control of SMB, this study employs an adjustable intelligent fuzzy controller with a structure like an approximate neural network (NN) for SMB control research. Simulation results demonstrate that the intelligent controller effectively achieves desirable control outcomes for the SMB system.

Keywords: chromatographic separation; SMB; multi-column; fuzzy; neural network

1. Introduction

It is known that the principle of chromatographic separation primarily relies on the equilibrium distribution of the molecules of the substances to be separated between the stationary and mobile phases. Different substances exhibit varying degrees of distribution between the two phases, resulting in different rates of movement with the mobile phase. Consequently, as the mobile phase moves, the various components within the mixture undergo mutual separation phenomena in the stationary phase.

SMB is a device used for liquid chromatographic separation based on the principle of adsorption. The mixture to be separated is first dissolved in a solvent and then injected into the column under high pressure. Each component is driven by the mobile phase and permeates through the stationary phase in the column. The extent of the movement of each component depends on its distribution state. Some components with weak interaction forces (adsorption forces) with the stationary phase

Preprints (www.preprints.org) | NOT PEER-REVIEWED | Posted: 7 November 2023 doi:10.20944/preprints202311.0420.v1

are quickly flushed out of the column, while others with stronger interaction forces take longer to elute. Chromatographic separation methods have been widely applied in the chemical and biomedical industries. Particularly in the biomedical sector, column chromatographic separation has become an important separation technique. Among these, the SMB technology, which allows continuous material separation, has garnered significant attention and usage due to its advantages of increased productivity and reduced solvent and water consumption. It is recognized as the cleanest manufacturing technology in the biopharmaceutical industry. Multi-column SMB, in particular, is deemed an indispensable technology in the separation and purification processes of the future biochemical pharmaceutical industry [1–3].

The operation of SMB primarily follows the concept of the traditional True Moving Bed (TMB) used in chemical engineering, as illustrated in Figure 1. When a feed containing two adsorbate components, A and B, enters a column filled with solid adsorbent and continuously flows upward, the adsorbate is absorbed by the solid. Subsequently, it is washed by the downflowing mobile phase, leading to the upward movement of component A, which has a stronger affinity, and the downward movement of component B, which has weaker retention.

By connecting several adsorption beds in series and setting up inlet and outlet points between adjacent bed bodies, including feed and sorbent inlets, as well as three outlets (extract, raffinate, and sorbent to recycle), the feed and withdrawal points are switched in a clockwise direction to the next position after a certain period. This simultaneous movement of all inlets and outlets results in a similar counterclockwise flow of the solid. Continuously changing the positions of the inlet and outlet points forms a counterclockwise flow of the solid adsorbent, while the mobile phase continues to flow clockwise, achieving continuous counter-current contact between the solid and the mobile phase, like the process in TMB.

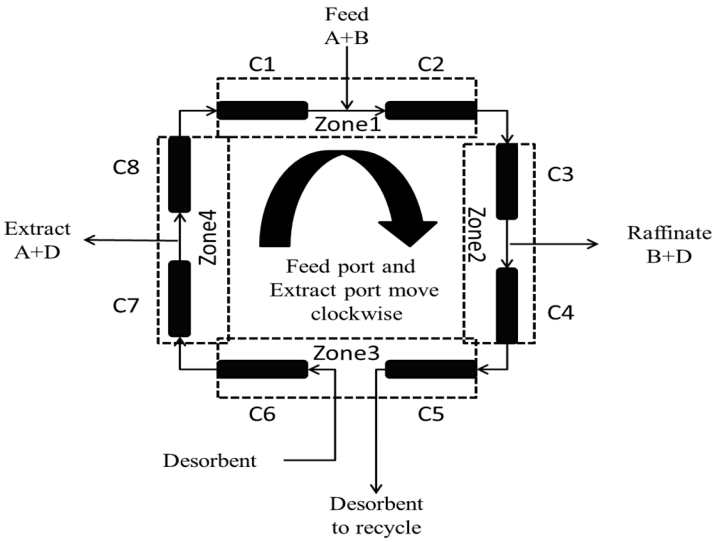

Figure 1. SMB Operation Process.

Although the simulated moving bed (SMB) has significantly improved the efficiency of chromatographic separation, its industrial application involves numerous parameters. Thus, determining the optimal parameters to control the separation process of SMB through practical trial-and-error experiments incurs substantial costs. Therefore, researchers in this field aim to conduct simulation-based quantitative analyses by studying the mathematical models of SMB. Currently, the mathematical models adopted by SMB primarily include the general rate model and the balanced diffusion model [4]. The general rate model is considered comprehensive in considering various factors and is closer to the actual process mechanism; however, it is overly complex. The balanced diffusion model is a slightly simplified mechanism model that can still effectively reflect the actual process when the concentration of separated components is relatively low [5]. Regarding the adopted isothermal equation form in the model, further subdivisions can be made [6].

 doi:10.20944/preprints202311.0420.v1

In the application of nonlinear control systems, the traditional design of nonlinear adaptive controllers is primarily based on the Lyapunov stability theorem. However, due to the highly nonlinear, sensitive, and discretely switched time parameters of the SMB system, it is challenging to find an appropriate Lyapunov function for such hybrid systems with discrete-time events. Designing a traditional nonlinear adaptive controller that can effectively control SMB is, therefore, a formidable task. Consequently, finding an effective and precise control method for multi-column SMB systems has been a longstanding goal in the field of biomedical and chemical applications.

It is known that fuzzy control has been widely applied in the nonlinear control field and finds practical use in industrial control. Its greatest advantage lies in its ability to achieve satisfactory control effects for unknown or partially known systems. Additionally, the learning capability of neural networks has demonstrated superior performance in the identification of unknown systems. Hence, this study aims to design an approximate neural network-like fuzzy controller for SMB control. This controller is expected to possess the capability to learn SMB system characteristics and modulate control parameters effectively. It is believed that this controller will contribute significantly to the practical application of SMB chromatographic separation.

2. Literature Review

For research into the control of complex nonlinear systems, with a focus on model-based studies rooted in both theoretical laboratory and practical applications, several control strategies are prominently involved. These include model predictive control (MPC), multi-level, multi-stage feedback control, and self-tuning control strategies. For instance, Klatt et al. introduced a model-based optimization control scheme for SMB chromatographic separations and its application in the separation of fructose and glucose [7]. Andrade Neto et al. presented a self-adjusting nonlinear MPC method for the enantiomeric separation of Praziquantel in an analog moving bed apparatus [8]. This control strategy aims to achieve efficient and accurate separation of Praziquantel enantiomers while maintaining the desired purity levels through real-time adjustments of control parameters. In both studies, the controllers successfully maintained the purity levels at the desired setpoints, achieving 99% purity in the extract and 98.6% purity in the residual solution.

Nogueira et al. have proposed a nominally stable MPC controller, also known as infinite horizon model predictive control (IHMPC), for the control of the simulated moving bed process applied to the separation of binaphthol enantiomers. This work lays the foundation for further advancements in the field of loop process dynamics and control [9]. Ju-Wen Lee introduced a simplified linear isothermal process model to estimate the process state of SMB chromatography. Within the moderately nonlinear range of the Langmuir isotherm, optimal setpoint conditions have been determined through a “one-switch-at-a-time” switching operation [10]. Yang et al. presented an optimization strategy based on an improved moving asymptote algorithm. [11]. Carols et al. proposed a method that combines wave theory and multi-model predictive control for the analysis and simulation of the dynamic characteristics of moving beds [12]. Suvarov et al. applied a self-regulating control strategy to adjust the purity and productivity of the raffinate, as well as the extraction flow rate, by modifying the spatial position of adsorption and desorption waves. This self-tuning control technology has been widely used in program-based control [13]. Maruyama et al. developed a multi-stage continuous control method for bypass simulated moving beds (BP-SMB) and demonstrated its feasibility through simulation results. The method effectively fits the set target yield value to the actual yield curve of the target substance and impurities [14].

In terms of simulating mobile bed optimization, Leibnitz et al. proposed a model-based optimization approach for the selection of an adsorbent in mobile bed processes. The method utilizes correlations between the structural properties of the adsorbent and the model parameters of a transport dispersive model [15]. Schulze et al. introduced the transient nonlinear wave propagation model (TWPM) for dynamic modeling of multi-component distillation columns with variable holdup. They demonstrated the applicability of this model for optimization and control purposes in single-section distillation columns and simple air separation units [16]. In terms of deep learning applications, Woo-Sung Lee and Chang-Ha Lee utilized limited experimental parameters and real

Preprints (www.preprints.org) | NOT PEER-REVIEWED | Posted: 7 November 2023 doi:10.20944/preprints202311.0420.v1

industrial data to develop mathematical dynamic models and data-driven machine learning approaches for evaluating SMB performance [17]. Marrocos et al. proposed a deep artificial intelligence structure with a nonlinear output error (NOE) structure and a nonlinear autoregressive with exogenous input (NARX) predictor. This structure serves as an online soft sensor to provide information on the main properties of a SMB chromatographic unit [18]. Hoon et al. applied a data-based deep Q network, which is a model-free reinforcement learning method, to train near-optimal control strategies for the SMB process [19]. This approach utilizes deep Q-networks and parallel numerical simulations to generate sufficient data for training control strategies for complex dynamic systems. For more details and further related studies, refer to the literature [20–27]. Typically, these studies are specific to particular equipment and separation materials rather than general solutions.

3. SMB Mathematical Discrete Model

Generally, traditional nonlinear model analysis primarily targets affine systems; however, the nonlinear nature of SMB exhibits three distinctive characteristics. (1) SMB control involves switching time parameters with discrete events, making it inherently more complex and nonlinear. (2) The control objective is not merely minimizing control output errors but rather ensuring that the component concentrations of the desired separated materials reach specific target ratios. In practical SMB operation, control parameters are often empirically determined. (3) SMB control variables exhibit strong coupling, and once control variables fall into an infeasible separation area, the system's output will appear uncontrollable.

In this study, firstly, the Crank-Nicolson method is employed for numerical computation of the SMB system to achieve more effective control. Secondly, the stability and error convergence of the discrete model are analyzed. Thirdly, sensitivity analysis of the regional velocity to pure monotonic intervals is conducted.

3.1. TMB and SMB Equation Model

The traditional SMB dynamic mathematical model is derived by referencing the TMB mathematical model. The definition of the parameters is presented in Table 1.

Here is an overview of the SMB dynamic model mentioned in the literature [17–19]. For the TMB, the mass balance of the bulk phase is given by:

$$\frac{\partial C_{ij}}{\partial t} = D_i \frac{\partial^2 C_{ij}}{\partial x^2} - v_j \frac{\partial C_{ij}}{\partial x} - \frac{1-\varepsilon}{\varepsilon} k_i (q_{ij}^* - q_{ij}) \tag{1}$$

$$\frac{\partial q_{ij}}{\partial t} = \frac{\partial}{\partial x} u_s q_{ij} + k_i (q_{ij}^* - q_{ij}) \tag{2}$$

Therefore, the TMB and SMB can be converted to each other using the following conversion:

$$\frac{\partial C_{ij}}{\partial t} = D_i \frac{\partial^2 C_{ij}}{\partial x^2} - v_j^* \frac{\partial C_{ij}}{\partial x} - \frac{1-\varepsilon}{\varepsilon} k_i (q_{ij}^* - q_{ij}) \tag{3}$$

Table 1. Parameters of SMB system.

Parameter	Nomenclature
$x(cm)$	Axial distance
$L(cm)$	Length column
$d(cm)$	Column diameter
$k_A(\mathrm{g}L^{-1})$	Comprehensive mass transfer constant of A
$k_B(\mathrm{g}L^{-1})$	Comprehensive mass transfer constant of B
H	Henry constant
$v^*(cm\,\mathrm{min}^{-1})$	Effect velocity of body
$u_s(cm\,\mathrm{min}^{-1})$	Solid flow rate

Preprints (www.preprints.org) | NOT PEER-REVIEWED | Posted: 7 November 2023 doi:10.20944/preprints202311.0420.v1

$C(gL^{-1})$	Mobile phase concentration
$q(gL^{-1})$	Solid phase concentration
$q^*(gL^{-1})$	Solid phase concentration at equilibrium between solid phase and mobile phase
$Q(cm^3\ \min^{-1})$	Volume flow rate
T	Switch time
$D(cm^2\ \min^{-1})$	Effective dispersion coefficient
ε	Bulk void fraction
i	Material index: A or B
j	Column number:1, 2, 3, 4, 5, 6, 7, 8

$$\frac{\partial q_{ij}}{\partial t} = k_i(q_{ij}^* - q_{ij}) \tag{4}$$

v_j^* is the velocity of SMB. Substituting equation (4) into equation (3), we obtain the following equation:

$$\frac{\partial C_{ij}}{\partial t} = D_i \frac{\partial^2 C_{ij}}{\partial x^2} - v_j^* \frac{\partial C_{ij}}{\partial x} - \frac{1-\varepsilon}{\varepsilon}\frac{\partial q_{ij}}{\partial t} \tag{5}$$

The adsorption equilibrium is represented by linear isotherms.

$$q_{ij} = H_i C_{ij} \tag{6}$$

The flow volume in each region must satisfy the following conditions：

$$\begin{aligned} &Q_I > Q_{IV}, Q_I > Q_{II}, Q_{III} > Q_{IV}, Q_{III} > Q_{IV} \\ &Q_I - Q_{IV} = Q_d, Q_I - Q_{II} = Q_x, Q_{III} - Q_{IV} = Q_r, Q_{III} - Q_{II} = Q_f \\ &v_j = \frac{Q_j}{\pi r^2} \end{aligned} \tag{7}$$

Q_d, Q_x, Q_r and Q_f are respectively the solvent, extract, raffinate and feed stream flow rates; they can also be selected as controllable variables. r represents the radius of column.

3.2. SMB Digitization by Crank-Nicolson Method

To achieve effective control of SMB, we conducted a numerical simulation analysis of the analogous substance diffusion process in the SMB system to perform a rigorous examination and verification.

Set $t_k = t_0 + ks$, $x_l = x_0 + lh$, $F = \frac{1-\varepsilon}{\varepsilon}$

$$\begin{aligned} \frac{\partial^2 C_{ij}}{\partial x^2} &= \frac{\frac{\partial^2 C_{ij}}{\partial x^2}|_{t_k} + \frac{\partial^2 C_{ij}}{\partial x^2}|_{t_{k+1}}}{2} \\ &= \frac{C_{ij}(x_{l-1}, t_{k+1}) - 2C_{ij}(x_l, t_{k+1}) + C_{ij}(x_{l+1}, t_{k+1}) + C_{ij}(x_{l-1}, t_k) - 2C_{ij}(x_l, t_k) + C_{ij}(x_{l+1}, t_k)}{2h^2} \end{aligned} \tag{8}$$

$$\begin{aligned} \frac{\partial C_{ij}}{\partial x} &= \frac{\frac{\partial C_{ij}}{\partial x}|_{t_k} + \frac{\partial C_{ij}}{\partial x}|_{t_{k+1}}}{2} \\ &= \frac{C_{ij}(x_{l+1}, t_{k+1}) - C_{ij}(x_{l-1}, t_{k+1}) + C_{ij}(x_{l+1}, t_k) - C_{ij}(x_{l-1}, t_k)}{4h} \end{aligned} \tag{9}$$

Preprints (www.preprints.org) | NOT PEER-REVIEWED | Posted: 7 November 2023 doi:10.20944/preprints202311.0420.v1

$$\frac{\partial C_{ij}}{\partial t} = \frac{C_{ij}(x_l, t_{k+1}) - C_{ij}(x_l, t_k)}{s} \tag{10}$$

$$\frac{\partial q_{ij}}{\partial t}(x_l, t_k) = H_i \frac{\partial C_{ij}}{\partial t}(x_l, t_k) \tag{11}$$

$$i = 1, \cdots M \ , \ j = 1, \cdots N$$

M, *N* represent respectively number of material and zones, here, *M*=2, *N*=8.
Substituting into the SMB system, $C_{ij}(x_l, t_k)$ denotes as $C_{ij}(l,k)$, and then we can get:

$$\begin{aligned}&(1+FH_i+\frac{Ds}{h^2})C_{ij}(l,k+1)-(\frac{vs}{4h}+\frac{Ds}{2h^2})C_{ij}(l-1,k+1)+(\frac{vs}{4h}-\frac{Ds}{2h^2})C_{ij}(l-1,k+1)\\&=(\frac{Ds}{2h^2}+\frac{vs}{4h})C_{ij}(l-1,k)+(1+FH_i-\frac{Ds}{h^2})C_{ij}(l,k)+(\frac{Ds}{2h^2}-\frac{vs}{4h})C_{ij}(l-1,k)\end{aligned} \tag{12}$$

With boundary conditions are:

$$C_{ij}(x,0) = C_{0ij} \tag{13}$$

$$\frac{\partial C_{ij}(x,t)}{\partial x}|_{x=l_s} = 0 \tag{14}$$

$$D_i \frac{\partial C_{ij}(x,t)}{\partial x}|_{x=0} = v_j[C_{ij}(0,t) - \bar{C}_{ij}^{sect}(t)] \tag{15}$$

C_{0ij} represents the initial concentration distribution inside the columns at *t*=0. In formulas (14) and (15), l_s and 0 represent, respectively, the end and initial position of the column. In a SMB arrangement, the column inlet concentration $\bar{C}_{ij}^{sect}(t)$ depends on the section and the location of the column within the section, as follows:

$$\bar{C}_{ij}^{\mathrm{I}}(t) = \frac{Q_{IV} C_{ij-1}(l_{n-1}, t)}{Q_I}, Section\ I,\ 1^{st}\ column$$

$$\bar{C}_{ij}^{\mathrm{III}}(t) = \frac{Q_{II} C_{ij-1}(l_{n-1}, t) + Q_f C_{fi}}{Q_{III}}, \quad Section\ III, 1^{st}\ column$$

$$\bar{C}_{ij}^{sect}(t) = C_{ij-1}(l_{n-1}, t), other \tag{16}$$

By using formulas (8-10), we can obtain the boundary numerate condition for the SMB system, involving the feed stream concentration C_f and the flow rate in each section (*Q*).

$$C_{ij}(n+1,k)+C_{ij}(n+1,k+1) = C_{ij}(n\text{-}1,k+1)+C_{ij}(n-1,k) \tag{17}$$

$$C_{ij}(2,k+1)+C_{ij}(2,k)-\frac{4hv_j}{D_i}(C_{ij}(1,k)-\bar{C}_{ij}^{sect}(k)) = C_{ij}(0,k+1)+C_{ij}(0,k) \tag{18}$$

Set $m = \frac{v^* s}{h}, n = \frac{Ds}{h^2}$, and from formula (12), we can get the equation (19).

Preprints (www.preprints.org) | NOT PEER-REVIEWED | Posted: 7 November 2023 doi:10.20944/preprints202311.0420.v1

$$\begin{aligned}&-(m+n)C_{ij}(l-1,k+1)+(1+FH_i+2n)C_{ij}(l,k+1)+(m-n)C_{ij}(l+1,k+1)\\&=(m+n)C_{ij}(l-1,k)+(1+FH_i-2n)C_{ij}(l,k)-(m-n)C_{ij}(l+1,k)\quad l\neq 1,n\end{aligned}\tag{19}$$

Substituting equations (17) and (18) into formula (12), we can get the next two boundary equations (20) and (21).

$$\begin{aligned}&(1+FH_i+2n)C_{ij}(1,k+1)-2nC_{ij}(2,k+1)\\&=(1+FH_i-2n-\frac{8m(m+n)}{n})C_{ij}(1,k)+2nC_{ij}(2,k)+\frac{8m(m+n)}{n}\bar{C}_{ij}^{sect}(k)\end{aligned}\tag{20}$$

$$-2nC_{ij}(n-1,k+1)+(1+FH_i+2n)C_{ij}(n,k+1)=2nC_{ij}(n-1,k)+(1+FH_i-2n)C_{ij}(n,k)\tag{21}$$

Denote the matric

$$A=\begin{bmatrix}1+FH_i+2n & -2n & 0 & \cdots & 0\\ -(m+n) & 1+FH_i+2n & (m-n) & \cdots & 0\\ \vdots & \vdots & \vdots & \vdots & \vdots\\ 0 & \cdots & -(m+n) & 1+FH_i+2n & (m-n)\\ 0 & \cdots & 0 & -2n & 1+FH_i+2n\end{bmatrix}$$

$$B=\begin{bmatrix}1+FH_i-2n-\frac{8m(m+n)}{n} & 2n & 0 & \cdots & 0\\ (m+n) & 1+FH_i-2n & -(m-n) & \cdots & 0\\ \vdots & \vdots & \vdots & \vdots & \vdots\\ 0 & \cdots & (m+n) & 1+FH_i-2n & -(m-n)\\ 0 & \cdots & 0 & 2n & 1+FH_i-2n\end{bmatrix}$$

$$w(k)=\begin{pmatrix}\frac{m^2}{m+n}\bar{C}_{ij}^{sect}(k) & 0 & \cdots & 0 & 0\end{pmatrix}^T$$

The iterative equation can be obtained as:

$$AC_{ij}(k+1)=BC_{ij}(k)+w(k)\tag{22}$$

3.3. Stability and Convergence Analysis

3.3.1. Stability Analysis

In the discussion of the stability of the Crank-Nicolson method applied to the SMB system, it is important to consider the source of errors in the process of digitalizing partial differential equations (PDEs). Two types of errors commonly arise: truncation errors resulting from derivative approximation and discretization, and error amplification inherent in the numerical method itself. To estimate truncation errors, the Taylor error formula can be employed, which provides an approximation of the error introduced by the discretization and derivative approximations. To explore error amplification, it is necessary to closely observe the behavior of the finite difference method. Von Neumann stability analysis is a technique commonly used to measure error amplification in numerical methods. The stability of the method requires selecting an appropriate step size or time increment to ensure that the amplification factor, as measured by Von Neumann stability analysis, does not exceed 1 for the $A^{-1}B$. By carefully considering the truncation errors and conducting the Von Neumann stability analysis with an appropriate step size, we can assess the

Preprints (www.preprints.org) | NOT PEER-REVIEWED | Posted: 7 November 2023 doi:10.20944/preprints202311.0420.v1

stability of the Crank-Nicolson method when applied to the specific equation of interest in the SMB system.

Let $C_{ij}^{*}(k)$ be the exact solution satisfying formula（22）and let $y_{ij}(k)$ be the approximate solution obtained by calculation and satisfying $Ay_{ij}(k+1)=By_{ij}(k)+w(k)$; the difference between them is $e_{ij}(k)=y_{ij}(k)-C_{ij}^{*}(k)$ satisfying

$$\begin{aligned} Ae_{ij}(k) &= Ay_{ij}(k)-AC_{ij}^{*}(k)=By_{ij}(k-1)+w(k-1)-(BC_{ij}^{*}(k-1)+w(k-1)) \\ &= Be_{ij}(k-1) \end{aligned} \tag{23}$$

If A is nonsingular, we can get the error iteration:

$$e_{ij}(k)=A^{-1}Be_{ij}(k-1) \tag{24}$$

In order to ensure that the error $e_{ij}(k)$ is not amplified, a spectral radius of $A^{-1}B$ must satisfy $\rho(A^{-1}B)<1$.

Theorem1: If matrix A is strictly diagonally dominant and it satisfies $|a_{ii}|>\sum_{\substack{j=1\\ j\neq i}}^{n}|a_{ij}|$, ($i$=1, 2,…, n), then matrix A is nonsingular.

Prove: If matrix A is a singular matrix, then there is a non-zero vector x that satisfies $Ax=0$. Set $|x_1|=\max\{|x_1|,|x_2|\cdots|x_n|\}$, $so\,|x_1|\neq 0$, we can get :

$$a_{11}x_1+a_{12}x_2+\cdots a_{1n}x_n=0,\ \ a_{11}=-a_{12}\frac{x_2}{x_1}-\cdots a_{1n}\frac{x_n}{x_1} \tag{25}$$

$$|a_{11}|\leq|a_{12}||\frac{x_2}{x_1}|+\cdots|a_{1n}||\frac{x_n}{x_1}|\leq\sum_{j=2}^{n}a_{1j} \tag{26}$$

This contradicts the condition, so matrix A is nonsingular.

Now let's review the matrix in the SMB iteration formula.

Because $A=\begin{bmatrix} 1+FH_i+2n & -2n & 0 & \cdots & 0 \\ -(m+n) & 1+FH_i+2n & (m-n) & \cdots & 0 \\ \vdots & \vdots & \vdots & \vdots & \vdots \\ 0 & \cdots & -(m+n) & 1+FH_i+2n & (m-n) \\ 0 & \cdots & 0 & -2n & 1+FH_i+2n \end{bmatrix}$

$$B=\begin{bmatrix} 1+FH_i-2n-\dfrac{8m(m+n)}{n} & 2n & 0 & \cdots & 0 \\ (m+n) & 1+FH_i-2n & -(m-n) & \cdots & 0 \\ \vdots & \vdots & \vdots & \vdots & \vdots \\ 0 & \cdots & (m+n) & 1+FH_i-2n & -(m-n) \\ 0 & \cdots & 0 & 2n & 1+FH_i-2n \end{bmatrix}$$

Let $m=\dfrac{v^{*}s}{h}=O(s), n=\dfrac{Ds}{h^2}=O(s)$, represent the infinitesimals of the same order. Provided that the time step is sufficiently small, matrices A and B exhibit strict diagonal dominance, rendering them nonsingular. Therefore, we can establish the stability of the iterative process involved in calculating the SMB system using the Crank-Nicolson method. By ensuring that the time step is small enough, the strict diagonal dominance of matrices A and B guarantees their nonsingularity, reinforcing the stability of the iterative process employed in the computation of the SMB system using the Crank-Nicolson method.

Preprints (www.preprints.org) | NOT PEER-REVIEWED | Posted: 7 November 2023 doi:10.20944/preprints202311.0420.v1

Theorem 2: If the space step (h) and time step (s) are both sufficiently small, $AC_{ij}(k+1) = BC_{ij}(k) + w(k)$ is stable.

Prove: Hypothesis λ is eigenvalue of $A^{-1}B$ and v is corresponding eigenvector. Select $\| v \|_{\infty} = 1$, the dimension of Matrix A is $p \times p$. So $| v_k | \leq 1, 1 \leq k \leq p$, choose component index $v_l = 1$. Indicators are divided into three situations:

(1) $2 \leq l \leq p-1$. According $A^{-1}Bv = \lambda v \Rightarrow Bv = \lambda Av$ so we can get the equation in component l:

$$(m+n)v_{l-1} + (1+FH-2n)v_l + (n-m)v_{l+1} = \lambda[-(m+n)v_{l-1} + (1+FH+2n)v_l + (m-n)v_{l+1}] \tag{27}$$

$$\text{If} | \lambda | = \frac{|(m+n)v_{l-1} + (1+FH-2n) + (n-m)v_{l+1}|}{|[-(m+n)v_{l-1} + (1+FH+2n) + (m-n)v_{l+1}]|} < 1 \tag{28}$$

Because $m = \frac{v^* s}{h} = O(s), n = \frac{Ds}{h^2} = O(s)$, so

$\forall \varepsilon > 0, \exists \delta, when\ s < \delta(h), can$ get $| m | \leq \varepsilon, | n | \leq \varepsilon$

For any s, select a space step h that is small enough to have $n > m \Rightarrow h < \frac{D}{v^*}$.

So, we get

$$(m+n)v_{l-1} + (n-m)v_{l+1} < 2n \tag{29}$$

For the split line over the fixed point (1, 1)

$$(m+n)v_{l-1} + (n-m)v_{l+1} = 2n \tag{30}$$

Rectangle $(v_{l-1}, v_{l+1}) \in [-1,1] \times [-1,1]$ (Figure 2) is under the split line, so it satisfies the inequality (29) except $(1,1)$ shown in Figure 2. Therefore, $| \lambda | \leq 1$ can be inferred.

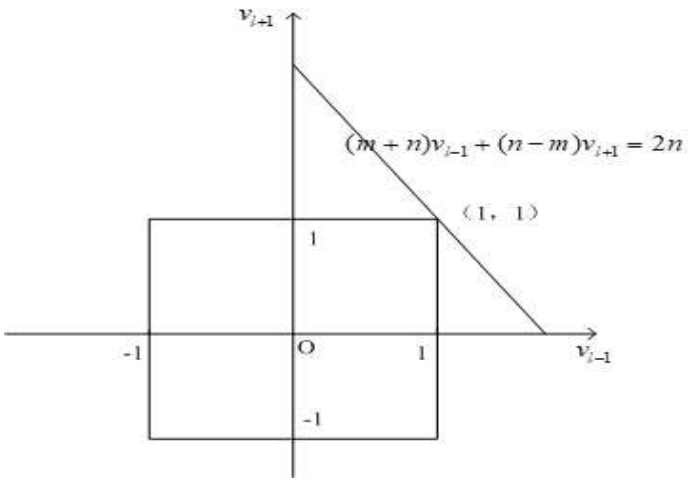

Figure 2. Space split line of (v_{l-1}, v_{l+1}).

Equality is established only if and only if $v_{l-1} = 1, v_{l+1} = 1$.

Now, it has been proven that if the components of the eigenvector meet this condition, contradictions arise for the previous component:

$$(m+n)v_{l-2} + (1+FH-2n)v_{l-1} + (n-m)v_l = [-(m+n)v_{l-2} + (1+FH-2n)v_{l-1} + (m-n)v_l] \tag{31}$$

Simplify equation (31), $v_{l-2} = 1$ can be obtained.

Preprints (www.preprints.org) | NOT PEER-REVIEWED | Posted: 7 November 2023 doi:10.20944/preprints202311.0420.v1

Any component can be obtained by the same principle, $v_k = 1, k = 1, \cdots p$.

But for the first component equation

$$(1 + FH - 2n - \frac{8m(m+n)}{n}) + 2n = (1 + FH + 2n) - 2n \Rightarrow \frac{8m(m+n)}{n} = 0$$

as $m = \frac{v^* s}{h} > 0, n = \frac{Ds}{h^2} > 0$, so $\frac{8m(m+n)}{n} > 0$, the statement contradicts the previous equation $\frac{8m(m+n)}{n} = 0$.

Thus, $|\lambda| < 1$

(2) $l = 1$, it means

$$(1 + FH - 2n - \frac{8m(m+n)}{n}) + 2nv_2 = \lambda[(1 + FH + 2n) - 2nv_2] \Rightarrow \quad (32)$$

$$\text{If } |\lambda| = \frac{(1 + FH - 2n - \frac{8m(m+n)}{n}) + 2nv_2}{(1 + FH + 2n) - 2nv_2} < 1 \quad (33)$$

$$v_2 < 1 + \frac{2m(m+n)}{n^2} \quad (34)$$

Because $\| v \|_\infty = 1$, so $|\lambda| < 1$

(3) $l = p$, it means

$$1 + FH - 2n + 2nv_{p-1} = \lambda[(1 + FH + 2n) - 2nv_{p-1}] \Rightarrow \quad (35)$$

$$\text{If} |\lambda| = \frac{1 + FH - 2n + 2nv_{p-1}}{[(1 + FH + 2n) - 2nv_{p-1}]} < 1 \quad (36)$$

$$v_{p-1} < 1 \quad (37)$$

When $v_{p-1} = 1 \Rightarrow \lambda = 1$

Now it has been proven that if the components of the eigenvector are in this situation, contradictions will occur.

$$(m + n)v_{l-2} + (1 + FH - 2n)v_{l-1} + (n - m)v_l = [-(m + n)v_{l-2} + (1 + FH - 2n)v_{l-1} + (m - n)v_l] \quad (38)$$

Like the first case, any component can be obtained by the same principle, $v_k = 1, k = 1, \cdots p$. So $|\lambda| < 1$ and be proved.

3.3.2 Convergence Analysis

Denote $\frac{\partial C_{ij}}{\partial x} = C_x, \frac{\partial^2 C_{ij}}{\partial x^2} = C_{xx}, , \frac{\partial^3 C_{ij}}{\partial x^3} = C_{xxx}, , \frac{\partial^4 C_{ij}}{\partial x^4} = C_{xxxx}, \frac{\partial C_{ij}}{\partial t} = C_t, \frac{\partial^2 C_{ij}}{\partial t^2} = C_{tt}$
$\frac{\partial^3 C_{ij}}{\partial t^3} = C_{ttt}, \frac{\partial^2 C_{ij}}{\partial x \partial t} = C_{xt}, \frac{\partial^3 C_{ij}}{\partial x^2 \partial t} = C_{xxt}, \frac{\partial^3 C_{ij}}{\partial x \partial t^2} = C_{xtt}, \frac{\partial^4 C_{ij}}{\partial x^2 \partial t^2} = C_{xxtt}$

According to the backward difference formula

Preprints (www.preprints.org) | NOT PEER-REVIEWED | Posted: 7 November 2023 doi:10.20944/preprints202311.0420.v1

$$C_t(l,k)=\frac{C(l,k)-C(l,k-1)}{s}+\frac{1}{2}sC_{tt}(l,k)-\frac{1}{6}s^2C_{ttt}(l,k_1),k_1\in(k-1,k)s \tag{39}$$

According to Taylor series expansion formula

$$C_{xx}(l,k-1)=C_{xx}(l,k)-sC_{xxt}(l,k)-\frac{1}{2}s^2C_{xxtt}(l,k_2),k_2\in(k-1,k)s \tag{40}$$

$$C_{xx}(l,k)=C_{xx}(l,k-1)+sC_{xxt}(l,k)+\frac{1}{2}s^2C_{xxtt}(l,k_2),k_2\in(k-1,k)s \tag{41}$$

By the central difference formula of the second derivative

$$C_{xx}(l,k)=\frac{C(l-1,k)-2C(l,k)+C(l+1,k)}{h^2}+\frac{h^2}{12}C_{xxxx}(l_1,k) \tag{42}$$

$$C_{xx}(l,k-1)=\frac{C(l-1,k-1)-2C(l,k-1)+C(l+1,k-1)}{h^2}+\frac{h^2}{12}C_{xxxx}(l_2,k-1) \tag{43}$$

$$l_1,l_2\in(l-1,l)h$$

$$C_x(l,k)=\frac{C(l+1,k)-C(l+1,k)}{2h}-\frac{h^2}{6}C_{xxx}(l_3,k) \tag{44}$$

$$C_x(l,k-1)=\frac{C(l-1,k-1)-C(l+1,k-1)}{2h}-\frac{h^2}{6}C_{xxx}(l_4,k-1) \tag{45}$$

$$C_x(l,k)=C_x(l,k-1)+sC_{xt}(l,k)+\frac{1}{2}s^2C_{xtt}(l,k_3),k_3\in(k-1,k)s \tag{46}$$

$$l_3,l_4\in(l-1,l)h$$

$$(1+FH)\frac{\partial C}{\partial t}=D\frac{\partial^2 C}{\partial x^2}-v\frac{\partial C}{\partial x} \tag{47}$$

Substituting equations (39), (41), (42), (43), (44), (45) into equation (47), we can get equation (48).

$$(1+FH)[\frac{C(l,k)-C(l,k-1)}{s}+\frac{1}{2}sC_{tt}(l,k)-\frac{1}{6}s^2C_{ttt}(l,k_1)]=$$

$$\frac{1}{2}D[\frac{C(l-1,k)-2C(l,k)+C(l+1,k)}{h^2}+\frac{h^2}{12}C_{xxxx}(l_1,k)]+\frac{1}{2}D[sC_{xxt}(l,k)+\frac{1}{2}s^2C_{xxtt}(l,k_2)]+$$

$$\frac{1}{2}D[\frac{C(l-1,k-1)-2C(l,k-1)+C(l+1,k-1)}{h^2}+\frac{h^2}{12}C_{xxxx}(l_2,k-1)]-$$

$$\frac{1}{2}v[\frac{C(l+1,k)-C(l+1,k)}{2h}-\frac{h^2}{6}C_{xxx}(l_3,k)]-\frac{1}{2}v[sC_{xt}(l,k)+\frac{1}{2}s^2C_{xtt}(l,k_3)+$$

$$\frac{C(l-1,k-1)-C(l+1,k-1)}{2h}-\frac{h^2}{6}C_{xxx}(l_4,k-1)] \tag{48}$$

Therefore, the error is the residual term after making the difference quotient, it equals to equation (48).

$$-\frac{1}{2}(1+FH)sC_{tt}(l,k)+\frac{1}{6}(1+FH)s^2C_{ttt}(l,k_1)+\frac{h^2}{24}D[C_{xxxx}(l_1,k)+C_{xxxx}(l_2,k-1)]+\frac{1}{2}DsC_{xxt}(l,k)+$$

Preprints (www.preprints.org) | NOT PEER-REVIEWED | Posted: 7 November 2023 doi:10.20944/preprints202311.0420.v1

$$\frac{1}{4}Ds^2C_{xxtt}(l,k_2)+\frac{vh^2}{12}[C_{xxx}(l_3,k)+C_{xxx}(l_4,k-1)]-\frac{1}{2}v[sC_{xt}(l,k)+\frac{1}{2}s^2C_{xtt}(l,k_3)] \quad (49)$$

For errors, the first-order expressions about space and time steps include:

$$-\frac{1}{2}(1+FH)sC_{tt}(l,k)+\frac{1}{2}DsC_{xxt}(l,k)-\frac{1}{2}vsC_{xt}(l,k).$$

By taking $\frac{\partial}{\partial t}$ for two sides of equation (47), we can get the following equation:

$$-\frac{1}{2}(1+FH)sC_{tt}(l,k)+\frac{1}{2}DsC_{xxt}(l,k)-\frac{1}{2}vsC_{xt}(l,k)=0 \quad (50)$$

So, the error tail term can be rewritten as:

$$\frac{1}{6}(1+FH)s^2C_{ttt}(l,k_1)+\frac{h^2}{24}D[C_{xxxx}(l_1,k)+C_{xxxx}(l_2,k-1)]+$$

$$\frac{1}{4}Ds^2C_{xxtt}(l,k_2)+\frac{vh^2}{12}[C_{xxx}(l_3,k)+C_{xxx}(l_4,k-1)]+\frac{1}{4}vs^2C_{xtt}(l,k_3) \quad (51)$$

Rearranging formula (51), can get formula (52):

$$[\frac{1}{6}(1+FH)C_{ttt}(l,k_1)+\frac{1}{4}DC_{xxtt}(l,k_2)+\frac{1}{4}vC_{xtt}(l,k_3)]s^2+$$

$$[\frac{D}{24}C_{xxxx}(l_1,k)+\frac{D}{24}C_{xxxx}(l_2,k-1)+\frac{v}{12}C_{xxx}(l_3,k)+\frac{v}{12}C_{xxx}(l_4,k-1)]h^2 \quad (52)$$

We conclude the error trail of Crank Nicolson is $O(h^2)+O(s^2)$.

4. Simulation

4.1. Experimental Environment and Data

In the simulated digitization system, there are 8 packed columns arranged in a 2-2-2-2 model. The initial parameters of the system are provided in Table 2. The time step is set to 0.1 second, and there are 50 spatial points for each column.

Table 2. The standard parameters for the separation.

Parameter	Value	Parameter	Value
$L(cm)$	25	$C_{f,i}(gL^{-1})$	5
$d(cm)$	0.46	$\theta(\min)$	3
H_A	0.001	$Q_I(cm^3\min^{-1})$	6.75
H_B	0.45	$Q_{II}(cm^3\min^{-1})$	6.6
$D_A(cm^2\min^{-1})$	0.2	$Q_{III}(cm^3\min^{-1})$	7
$D_B(cm^2\min^{-1})$	1.265	$Q_{IV}(cm^3\min^{-1})$	2
ε	0.8	spatial number	50

The research experiments were conducted using the MATLAB R2016a software on a PC equipped with an Intel Core i7-3770K 3.53GHz processor and 16GB RAM. The experimental data was

Preprints (www.preprints.org) | NOT PEER-REVIEWED | Posted: 7 November 2023 doi:10.20944/preprints202311.0420.v1

generated based on simulated experiments, resulting in a data volume of 70MB. The separation process of SMB without any control conditions shown in Figure 3.

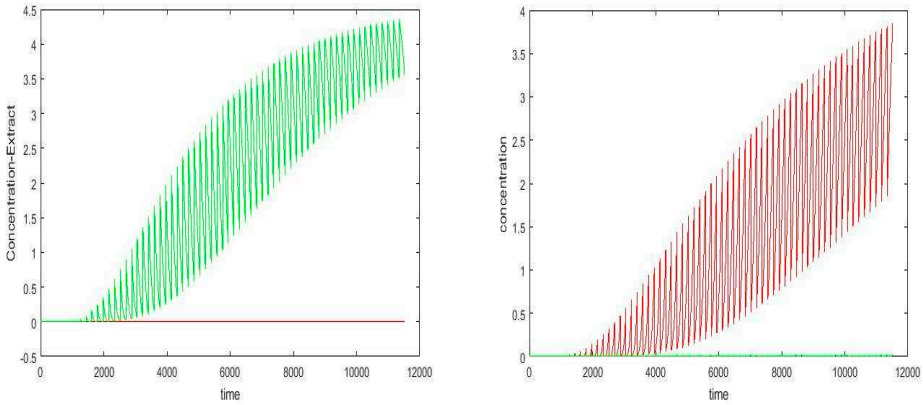

Figure 3. Concentration of the SMB process on extract and raffinate.

4.2. Sensitivity Analysis of Purity Flow Rates to Find Local Monotonic Intervals

In Figure 4, Q_I change from 7.32 to 7.5, and when Q_{II} = 6.96, Q_{III} = 8.4, Q_{IV} = 2 remain unchanged, the switch time is 180 seconds. The purity of extract solution for material B decreases with the increase of the flow rate in Zone I. However, the concentration of raffinate for material A remains almost unchanged.

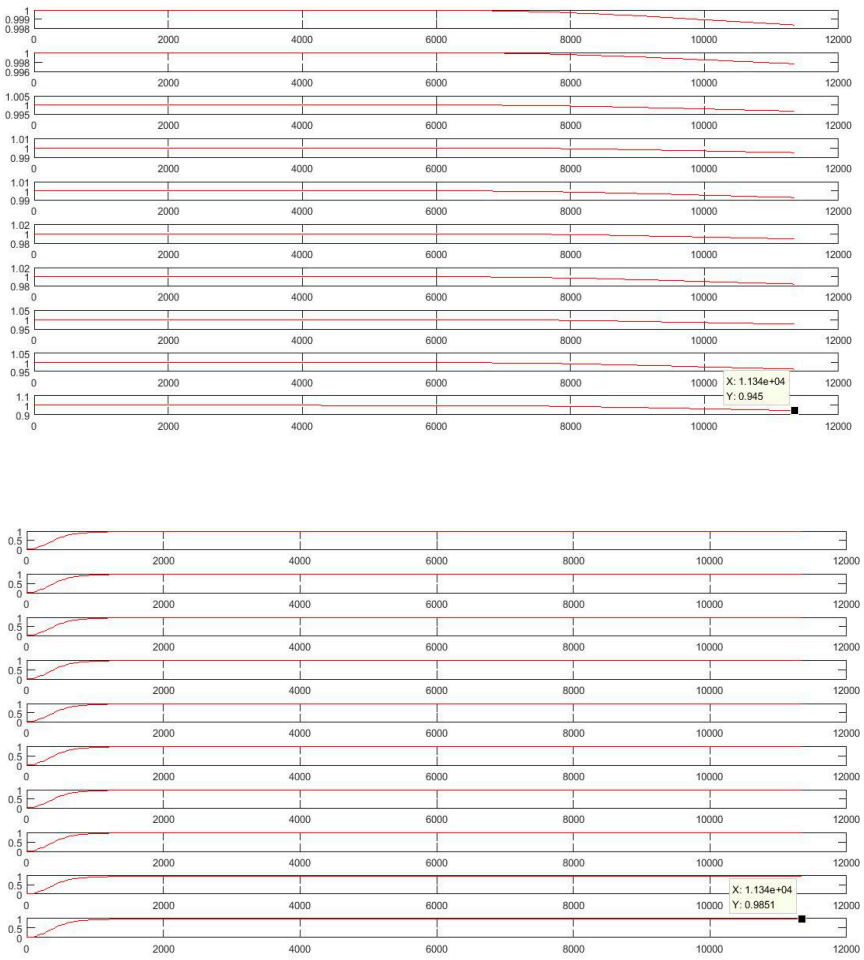

Figure 4. The influence of Zone I flow rate on purity.

Preprints (www.preprints.org) | NOT PEER-REVIEWED | Posted: 7 November 2023 doi:10.20944/preprints202311.0420.v1

In Figure 5, Q_{II} changes from 6.92 to 7.1, when Q_I = 7.14, Q_{III} = 8.4, Q_{IV} = 2 and the switch time is 180 seconds. The purity of the extract solution of material B remains almost unchanged as the flow rate of Zone II increases, but the purity of raffinate for material A decreases with an increase in the flow rate of Q_{II}.

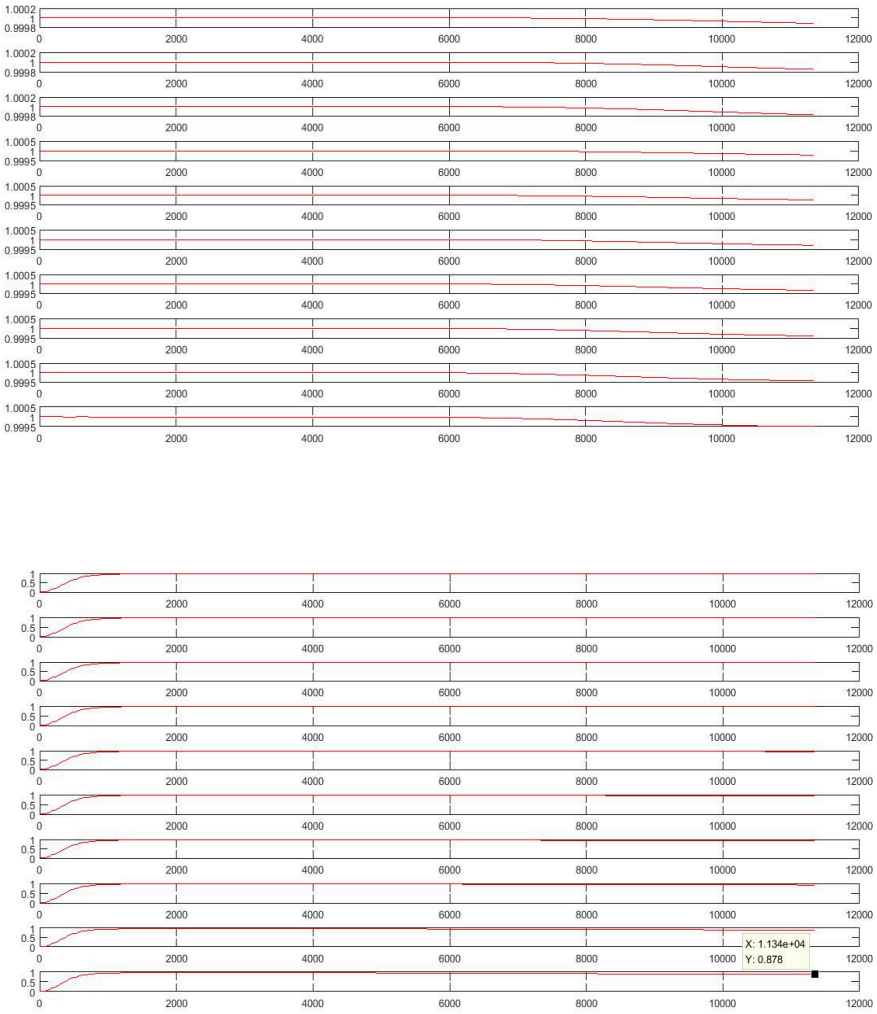

Figure 5. The influence of Zone II flow rate on purity.

In Figure 6, Q_{III} changes from 8.4 to 12, when Q_I = 6.96, Q_{II} = 7.2, Q_{IV} = 2 and the switch time is 180 seconds. The purity of extract solution of material B decreases with an increase of Zone III flow. Similarly, the purity of raffinate of material A decreases with the increase of Zone III flow. But decrease tendency is very small, so it is better for fine tuning. However, whether it is material A or material B, the change amount is relatively small, so the flow rate in this area suitable for fine-tuning control.

Preprints (www.preprints.org) | NOT PEER-REVIEWED | Posted: 7 November 2023 doi:10.20944/preprints202311.0420.v1

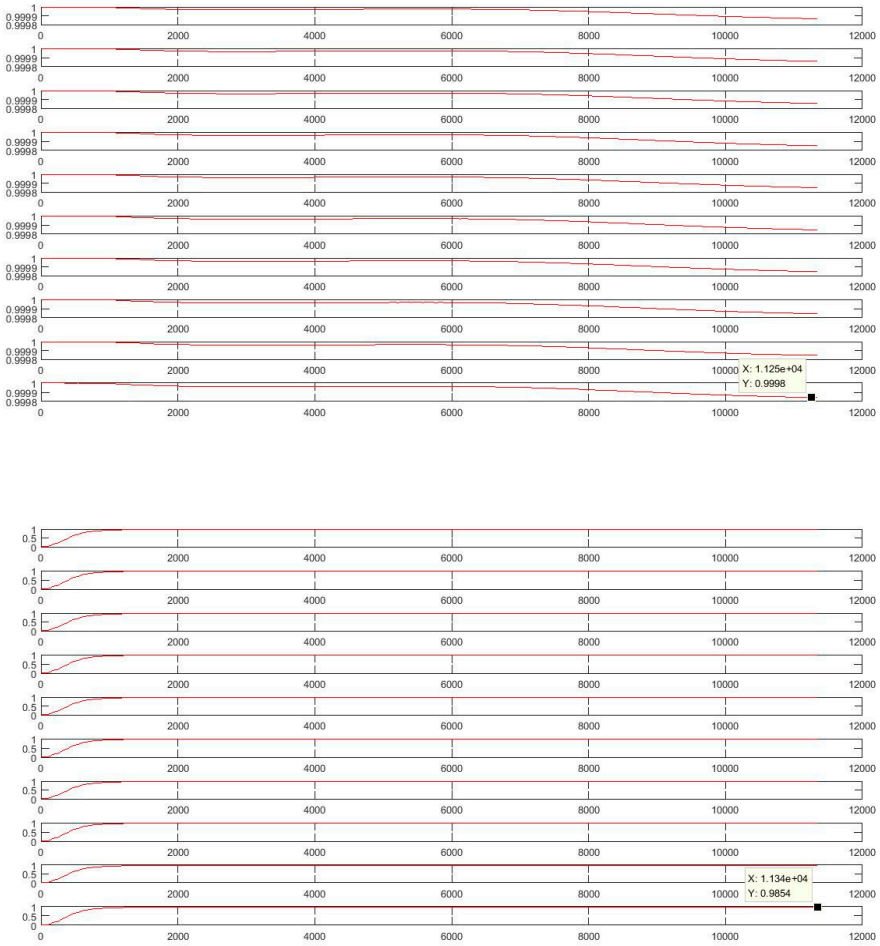

Figure 6. The influence of Zone III flow rate on purity.

In Figure 7, Q_{IV} changes from 2.2 to 4, when Q_I = 7.2, Q_{II} = 6.96, Q_{III} = 10 and the switch time is 180 seconds. In the system, both the purity of extract for material B and the purity of raffinate for material A decrease with an increase in the Zone IV flow rate. However, the decline is relatively small. Therefore, fine-tuning the system parameters may be beneficial to achieve the desired purity levels.

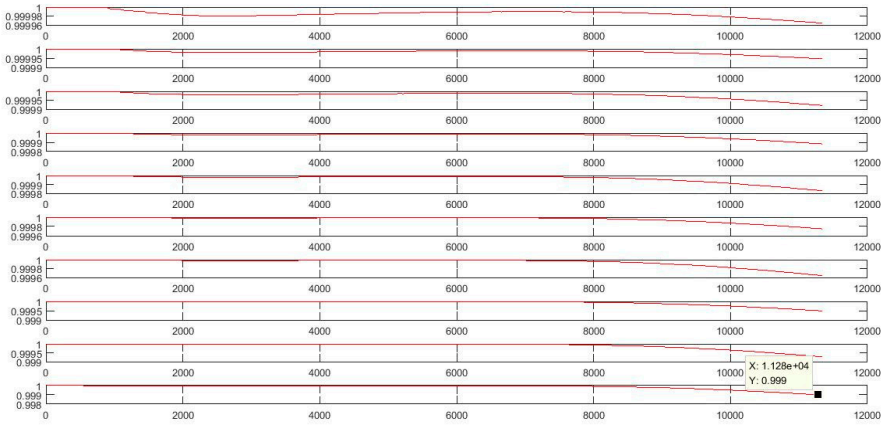

Preprints (www.preprints.org) | NOT PEER-REVIEWED | Posted: 7 November 2023 doi:10.20944/preprints202311.0420.v1

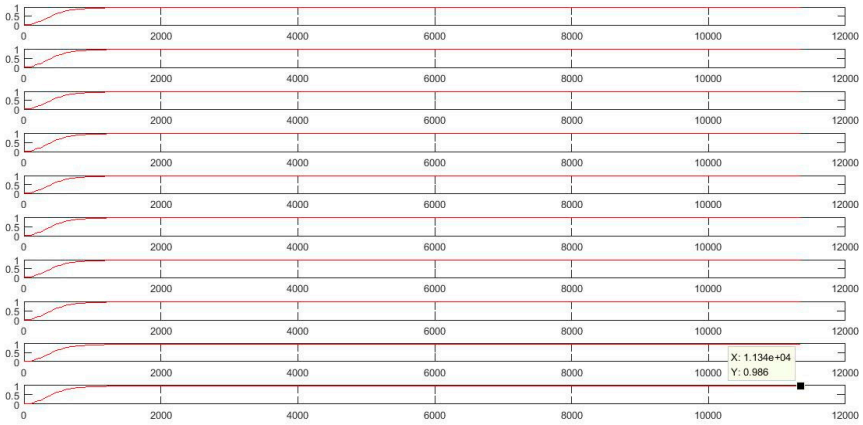

Figure 7. The influence of Zone IV flow rate on purity.

5. Smart Controller Design

As mentioned before, SMB is a very complex nonlinear system. The control of a multi-column SMB system cannot be accomplished independently by one controller. Each feed hole must be equipped with an independent controller for control. The purpose of chromatographic separation can only be achieved through precise and appropriate feed speed control of the flow rate of the material to be separated. Therefore, how to design a smart controller with learning and self-adjustment abilities is another aim of this study in SMB control applications. In view of this, the smart controller designed in this research combines the characteristics of fuzzy control and neural network (NN) control. It is a NN-like fuzzy controller. It adopts the concept of "ANFIS: adaptive-network-based fuzzy inference system" proposed by J-S.R. Jang as the controller architecture [28,29].

5.1. Fuzzy Rule Control and Hierarchical Design

First, several symbolic meanings in the control are defined as follows.

$$\Delta e(k) = e(k) - e(k-1) \tag{53}$$

$$\Delta e(k\text{-}1) = e(k\text{-}1) - e(k-2) \tag{54}$$

$$e(k) = desired\ \ output - y(k) \tag{55}$$

In the SMB control system, the fuzzy input variables are selected as error ($e(k)$) and error change ($\Delta e(k)$), the formula is as follows:

$e_1(k)$ = B material desired output– $C_{E,B}$ (56)

$e_2(k)$ = A material desired output – $C_{R,A}$ (57)

$$\Delta e_1(k) = e_1(k) - e_1(k-1) \tag{58}$$

$$\Delta e_2(k) = e_2(k) - e_2(k-1) \tag{59}$$

In the smart controller mechanism, the control output is the liquid flow rate increment. The selected input fuzzy variables are error and error change. The fuzzy system defines five linguistic variable values for error and error change, respectively: NB, NS, ZE, PS, and PB. The graph of the membership function is shown in Figure 8.

Preprints (www.preprints.org) | NOT PEER-REVIEWED | Posted: 7 November 2023 doi:10.20944/preprints202311.0420.v1

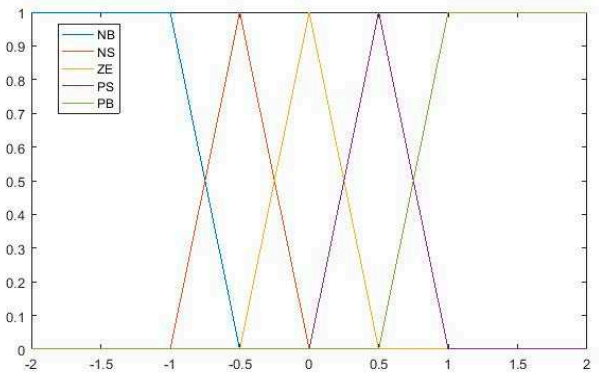

Figure 8. Membership function of e(k) and Δe(k).

In the subsequent SMB control process, the increments of the flow rate Q_I in region I, Q_{II} in region II, and Q_{III} in region III are chosen as three independent defuzzification output variables denoted as ΔQ_i $(i=1,2,3)$ respectively. The membership function of ΔQ_i is shown in Figure 9.

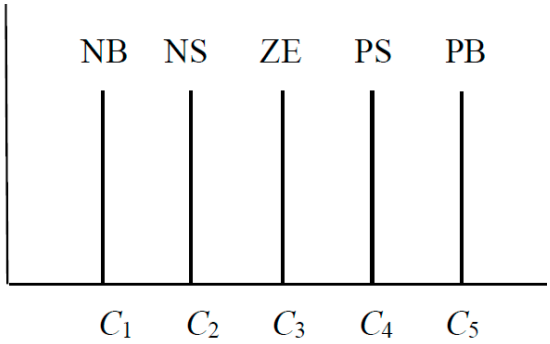

Figure 9. Membership function of ΔQ_i (*i*=1, 2, 3).

Since purity decreases with an increase in flow rate, the values of (C_1, C_2, C_3, C_4, C_5) are set as { -0.15, -0.1, 0, 0.1, 0.15} for ΔQ_1, {-0.006, -0.004, 0, 0.0.004, 0.006} for ΔQ_2 and {-0.08, -0.05, 0, 0.05, 0.08} for ΔQ_3. When conducting sensitivity analysis near the flow rate region, it is necessary to adjust the rule table to reflect the decrease in purity with the increasing flow rate. Thus, the rule table was developed as listed in Table 3.

Although the system is a multiple input and multiple output (MIMO) system, there is no coupling between the velocity in the first region and the velocity in the second region. Additionally, the flow velocity in the third region can be fine-tuned independently. This allows for the execution of the control process sequentially in the design control process.

Table 3. Rule table of ΔQ_i (*i*=1, 2, 3).

Δe \ e	*NB*	*NS*	*ZE*	*PS*	*PB*
NB	*PB*	*PB*	*PB*	*PS*	*NB*
NS	*PB*	*PS*	*PS*	*ZE*	*NB*
ZE	*PB*	*PS*	*ZE*	*NS*	*NB*
PS	*PB*	*ZE*	*NS*	*NS*	*NB*

Preprints (www.preprints.org) | NOT PEER-REVIEWED | Posted: 7 November 2023 doi:10.20944/preprints202311.0420.v1

PB	*PB*	*NS*	*NB*	*NB*	*NB*

In the preceding part of the reasoning, the Mamdani operator, basic complementary operation, and Mamdani fuzzy reasoning rule are utilized. The velocity in Zone I primarily affects the purity of the extract material B, while the velocity in Zone II mainly influences the purity of the raffinate material A. The effect of Zone IV's velocity is similar to that of Zone III; hence, Zone III's velocity is selected as the control variable. The action diagrams of the three independent controllers are shown in Figure 10.

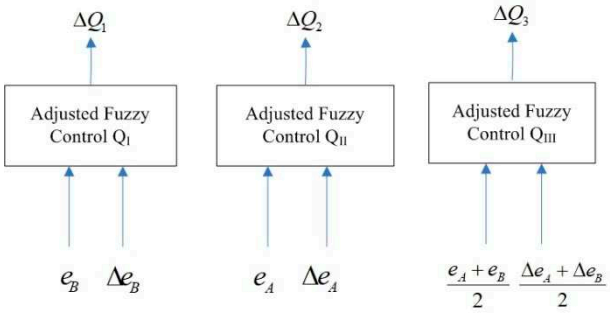

Figure 10. Three independent controllers.

5.2. NN-like Fuzzy Controller Framework

The NN-like fuzzy controller is divided into five layers, as shown in Figure 11. The functions of each layer are described below.

Layer1: This layer calculates the values of the fuzzy membership function corresponding to the input variables, including the error and error change. u_{A_i} represents the error membership function values, u_{B_i} represents the error change membership function value.

Layer2: In this layer, the starting strength of rule base is calculated according to the fuzzy rule base. Z_i represents the starting strength.

$$\begin{aligned} Z_1 &= u_{A_1} * u_{B_1} \\ Z_2 &= u_{A_1} * u_{B_2} \\ &\vdots \\ Z_{24} &= u_{A_5} * u_{B_4} \\ Z_{25} &= u_{A_5} * u_{B_{25}} \end{aligned} \tag{60}$$

Layer 3: The third layer performs the regularization operation of fuzzy start-up intensity. W_{nm} stands for connection weight, and net_n represents regularization output fuzzy start-up intensity.

$$net_n = \frac{Z_n * W_{nn}}{\sum_{m=1}^{25} Z_m * W_{nm}}, n = 1, 2, 3 \cdots 25 \tag{61}$$

Preprints (www.preprints.org) | NOT PEER-REVIEWED | Posted: 7 November 2023 doi:10.20944/preprints202311.0420.v1

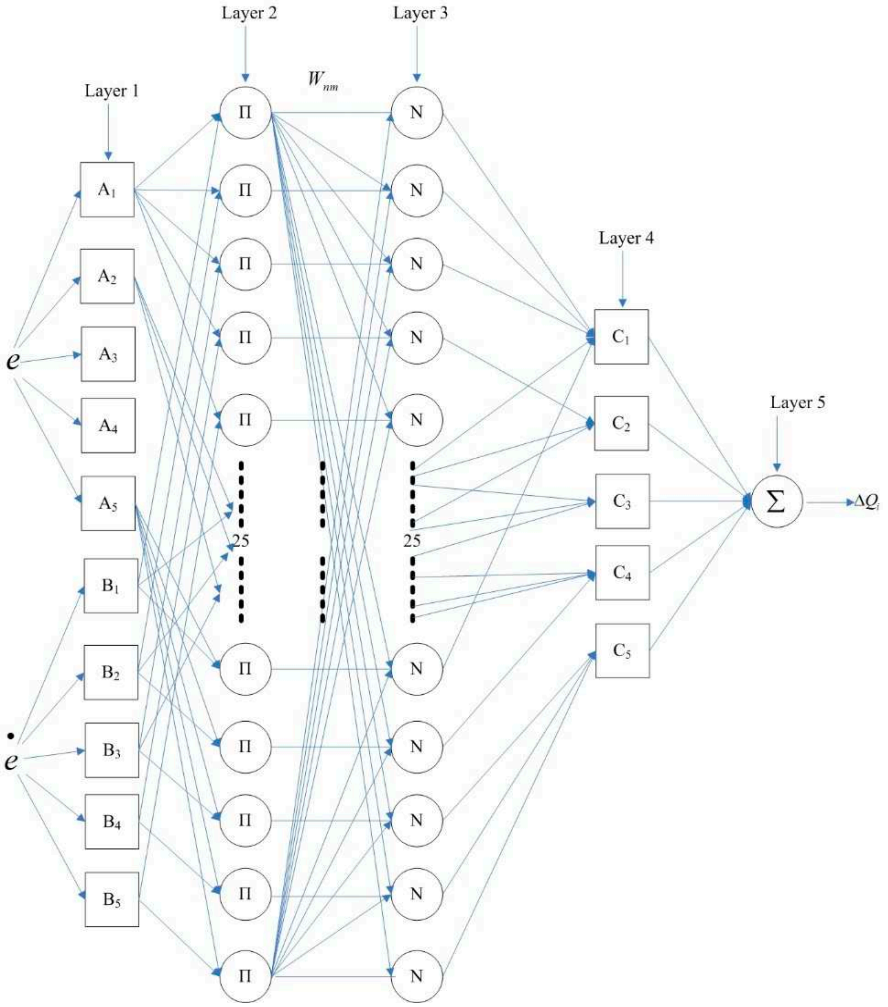

Figure 11. NN-like fuzzy controller framework.

Layer 4: This layer calculates the startup of the IF part after the regularization operation of the fuzzy rules. net_n is the input of this layer, $O_{4,n}$ is the output of this layer, and C_{n_k} indicates that the layer is a shared weight.

$$O_{4,n} = net_n * C_{n_k} \tag{62}$$

$$C_1{=}C_{NB}, C_2{=}C_{NS}, C_3{=}C_{ZE}, C_4{=}C_{PS}, C_5{=}C_{PB} \tag{63}$$

Layer 5: This layer calculates the final control output of the neuron.

$$\Delta u = \sum_{n=1}^{25} net_n * C_{n_k} \tag{64}$$

Updating weights using back-propagation algorithms similar to neural networks，it can get the updating formulas as follows:

Set loss function: $E = \frac{1}{2}(desired - y)^2$ (65)

$$\delta_o = -\frac{\partial E}{\partial y}\frac{\partial y}{\partial u}\frac{\partial u}{\partial \Delta u} = (desire - y) * \mathrm{sgn}\left(\frac{y(t) - y(t-1)}{u(t) - u(t-1)}\right) * 1 \tag{66}$$

Preprints (www.preprints.org) | NOT PEER-REVIEWED | Posted: 7 November 2023 doi:10.20944/preprints202311.0420.v1

$$\frac{\partial E}{\partial C_1}=\frac{\partial E}{\partial y}\frac{\partial y}{\partial u}\frac{\partial u}{\partial \Delta u}\frac{\partial \Delta u}{\partial C_1}=-\delta_o*(net_1+net_2+net_3+net_6+net_{11}+net_{16}+net_{21}) \quad (67)$$

$$\frac{\partial E}{\partial C_2}=\frac{\partial E}{\partial y}\frac{\partial y}{\partial u}\frac{\partial u}{\partial \Delta u}\frac{\partial \Delta u}{\partial C_2}=-\delta_o*(net_4+net_7+net_8+net_{12}) \quad (68)$$

$$\frac{\partial E}{\partial C_3}=\frac{\partial E}{\partial y}\frac{\partial y}{\partial u}\frac{\partial u}{\partial \Delta u}\frac{\partial \Delta u}{\partial C_3}=-\delta_o*(net_9+net_{13}+net_{17}) \quad (69)$$

$$\frac{\partial E}{\partial C_4}=\frac{\partial E}{\partial y}\frac{\partial y}{\partial u}\frac{\partial u}{\partial \Delta u}\frac{\partial \Delta u}{\partial C_4}=-\delta_o*(net_{14}+net_{18}+net_{19}+net_{22}) \quad (70)$$

$$\frac{\partial E}{\partial C_5}=\frac{\partial E}{\partial y}\frac{\partial y}{\partial u}\frac{\partial u}{\partial \Delta u}\frac{\partial \Delta u}{\partial C_5}=-\delta_o*(net_5+net_{10}+net_{15}+net_{20}+net_{23}+net_{24}+net_{25}) \quad (71)$$

$$\Delta C_n=\eta*\frac{\partial E}{\partial C_n} \quad (72)$$

η is learning rate

$$\frac{\partial E}{\partial W_{nm}}=\frac{\partial E}{\partial y}\frac{\partial y}{\partial u}\frac{\partial u}{\partial \Delta u}\frac{\partial \Delta u}{\partial net_n}\frac{\partial net_n}{\partial W_{nm}} \quad (73)$$

$$\delta_n=\delta_o*C_{n_k} \quad (74)$$

$$\frac{\partial E}{\partial W_{nm}}=-\delta_n*\frac{Z_n*\sum_{m=1}^{25}Z_m*W_{nm}-Z_m*Z_n*W_{nn}}{(\sum_{m=1}^{25}Z_m*W_{nm})^2},m=n \quad (75)$$

$$\frac{\partial E}{\partial W_{nm}}=-\delta_n*\frac{-Z_m*Z_n*W_{nn}}{(\sum_{m=1}^{25}Z_m*W_{nm})^2},m\neq n \quad (76)$$

$$\Delta W_{nm}=\eta*\frac{\partial E}{\partial W_{nm}} \quad (77)$$

6. SMB Control Experiments

6.1. Purity Control Result

To verify the applicability of the NN-like fuzzy controllers in SMB control, we conducted several experiments on the purity control of the SMB system. Figures 12–18 show the effects of material separation results for materials *A* and *B* located at the outlets of the extraction (material *B*) and raffinate (material *A*).

Preprints (www.preprints.org) | NOT PEER-REVIEWED | Posted: 7 November 2023 doi:10.20944/preprints202311.0420.v1

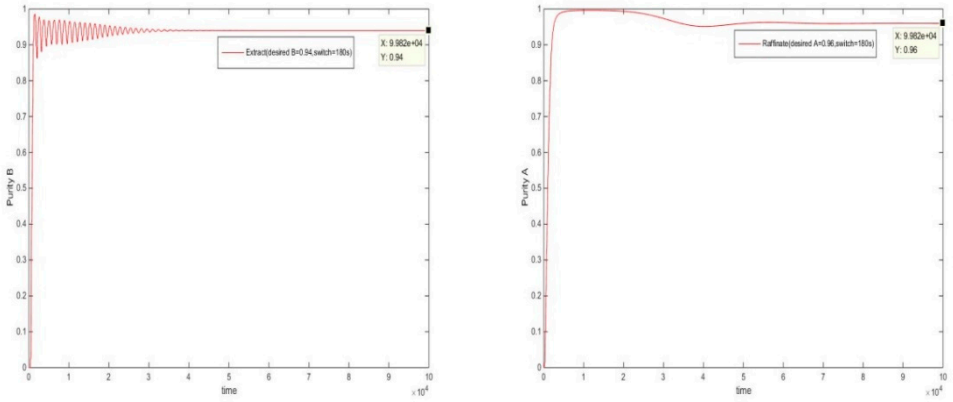

Figure 12. Purity control of the first experiment (switch time=180s). (actual *B*=94%, desired *B*=94%, actual *A*=96%, desired *A*=96%).

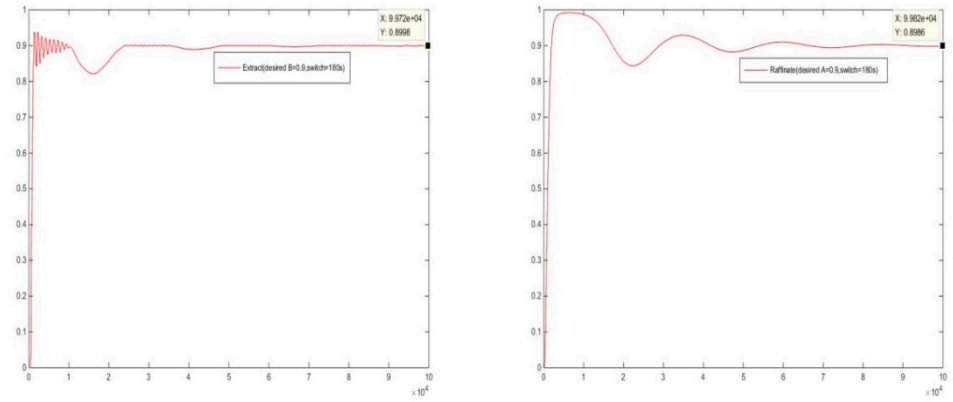

Figure 13. Purity control of the second experiment (switch time=180s). (actual *B*=89.98%, desired *B*=90%, actual *A*=89.86%, desired *A*=90%).

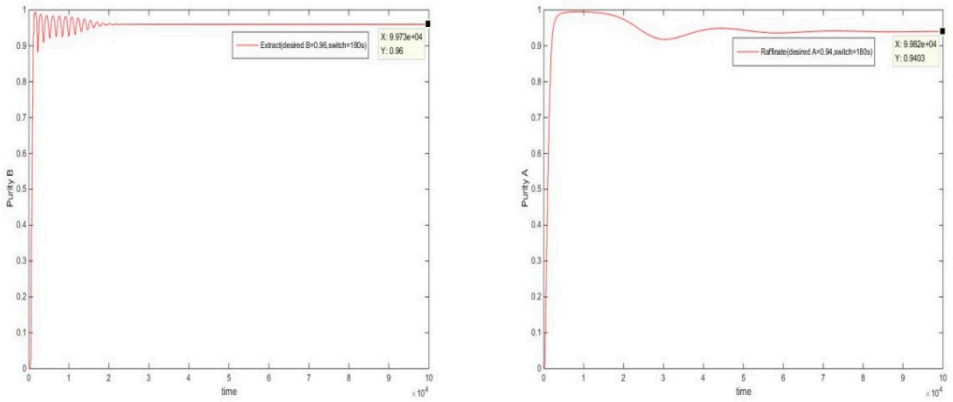

Figure 14. Purity control of the third experiment (switch time=180s). (actual *B*=96%, desired *B*=96%, actual *A*=94.03%, desired *A*=94%).

Preprints (www.preprints.org) | NOT PEER-REVIEWED | Posted: 7 November 2023 doi:10.20944/preprints202311.0420.v1

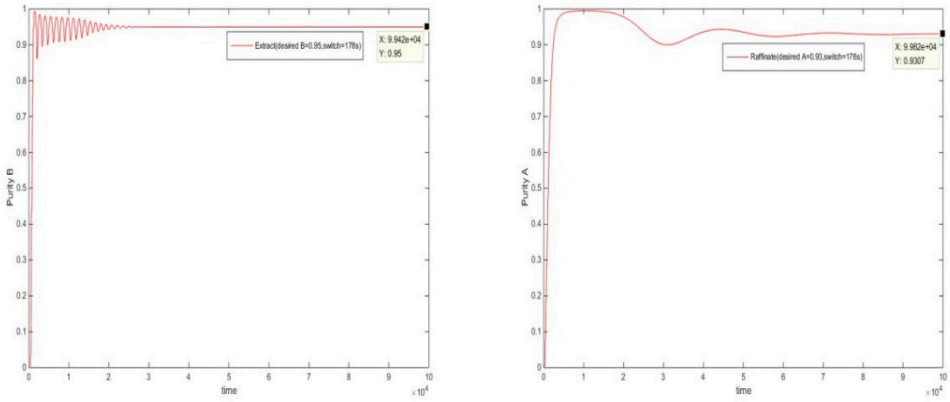

Figure 15. Purity control of the fourth experiment (switch time=178s). (actual *B*=95%, desired *B*=95%, actual *A*=93.07%, desired *A*=93%).

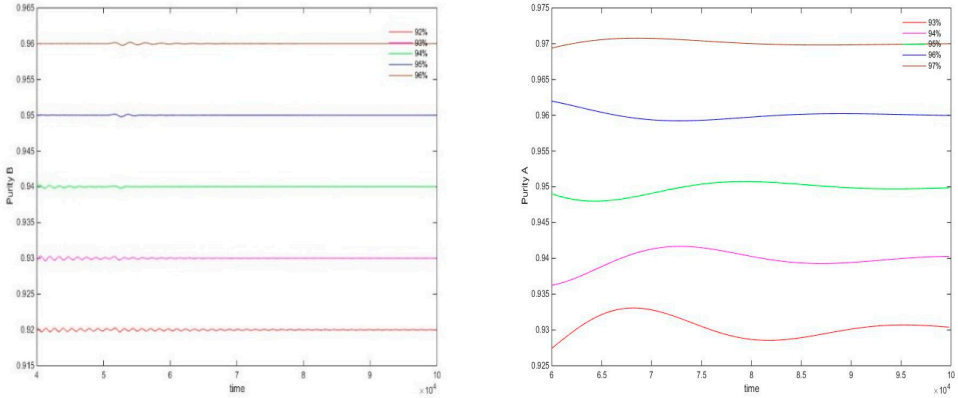

Figure 16. Control effects under the disturbance of adsorbent parameter.

$$H_A = 0.01 \rightarrow 0.03$$

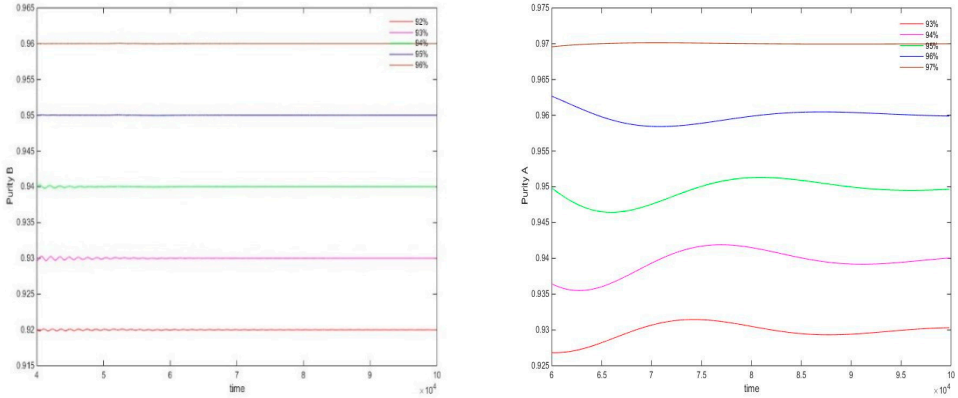

Figure 17. Control effects under the disturbance of feed port concentration.

$$C_f = 4.5 \rightarrow 5.2$$

Preprints (www.preprints.org) | NOT PEER-REVIEWED | Posted: 7 November 2023 doi:10.20944/preprints202311.0420.v1

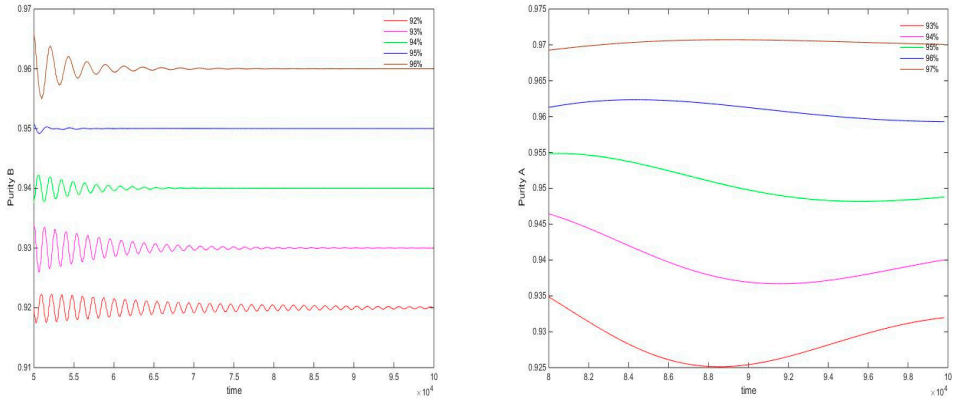

Figure 18. Control effects under the disturbance of switch time.

$$\theta = 178s \rightarrow 182s$$

From Figures 12–15, it is evident that the NN-like fuzzy controller performs with high accuracy in controlling the purity of the extraction and raffinate outlet materials. The steady-state error in controlling the purity of the extraction solution's outlet material and the raffinate solution's outlet material is nearly negligible. Furthermore, Figures 16–18 show that the controller exhibits stability in the face of various disturbances, such as changes in adsorbent parameters, inlet concentration, and switching time.

6.2. Controller Comparison

In order to demonstrate that the NN-like fuzzy controller has excellent robustness and adaptability in SMB control compared with the traditional fuzzy controller, we also conducted an experimental comparison of the two controllers.

From Figures 19–21, it is evident that the NN-like fuzzy controller outperforms the traditional fuzzy controller. In comparison to the traditional fuzzy controller, the NN-like fuzzy controller exhibits superior performance. Specifically, when considering the purity of substance *B* at the outlet of extraction, the traditional fuzzy controller shows steady-state errors and fluctuations, whereas the NN-like fuzzy controller maintains stability without any steady-state errors throughout. There is no significant difference in the control effect for the concentration of substance at the raffinate outlet. However, when the switching time is changed to 178 seconds, the traditional fuzzy controller displays ill-conditioned characteristics. This is because it does not adjust the membership function of the force intensity of the control force or the center value of the force output. On the other hand, the NN-like fuzzy controller remains robust and unaffected by the switching time disturbance.

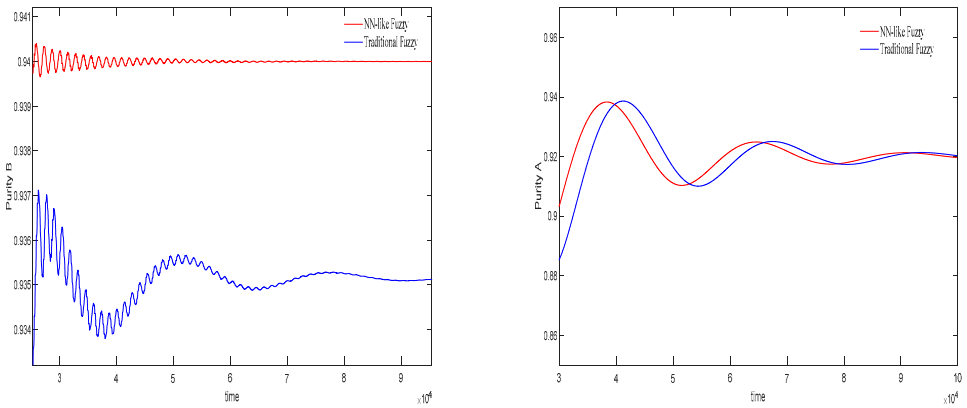

Figure 19. Comparison of two controllers (desired *B*=94%, desired *A*=92%, switch time=180s).

Preprints (www.preprints.org) | NOT PEER-REVIEWED | Posted: 7 November 2023 doi:10.20944/preprints202311.0420.v1

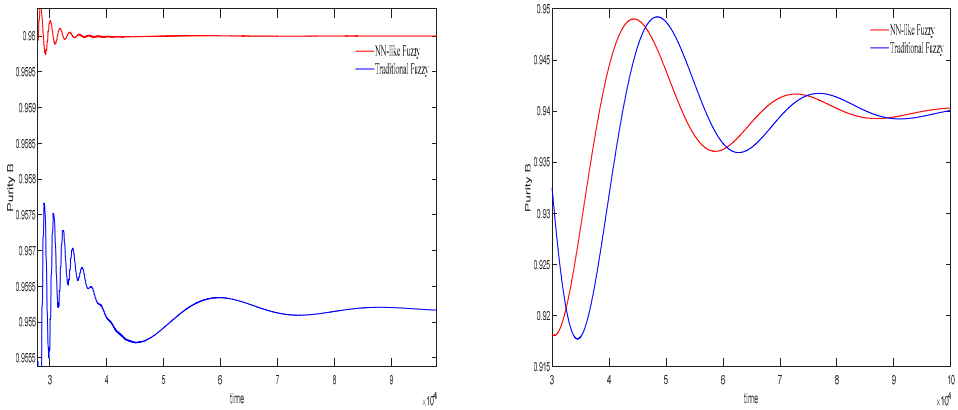

Figure 20. Comparison of two controllers (desired *B*=96%, desired *A*=94%, switch time=180s).

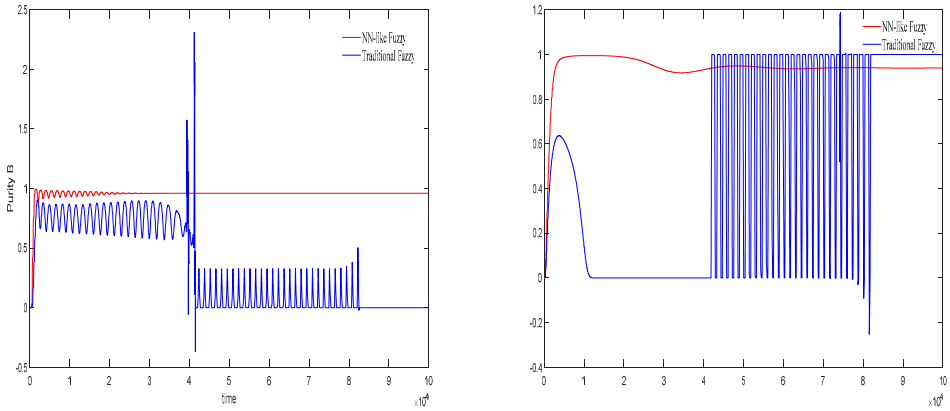

Figure 21. Comparison of two controllers (desired *B*=96%, desired *A*=94%, switch time=178s).

In Figures 22–24, both controllers demonstrate the ability to maintain stability under the disturbance of adsorbent parameters and inlet concentration variations. However, the NN-like fuzzy controller exhibits higher stability compared to the traditional fuzzy controller. Furthermore, when faced with the disturbance of switching time with high sensitivity, the traditional fuzzy controller once again exhibits ill-conditioned features, while the NN-like fuzzy controller remains robust. Therefore, the NN-like fuzzy controller proves to be a robust and adaptive solution for highly complex and sensitive SMB systems.

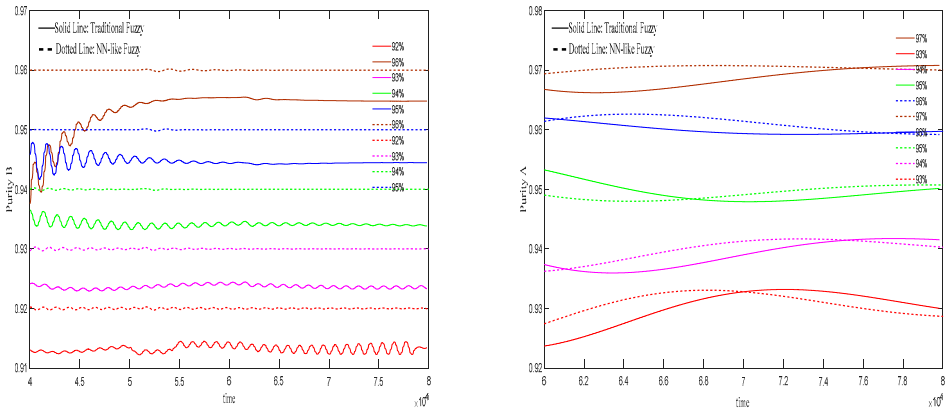

Figure 22. Comparison of two controllers under the disturbance of adsorbent parameters.

$$H_A = 0.01 \rightarrow 0.03$$

Preprints (www.preprints.org) | NOT PEER-REVIEWED | Posted: 7 November 2023 doi:10.20944/preprints202311.0420.v1

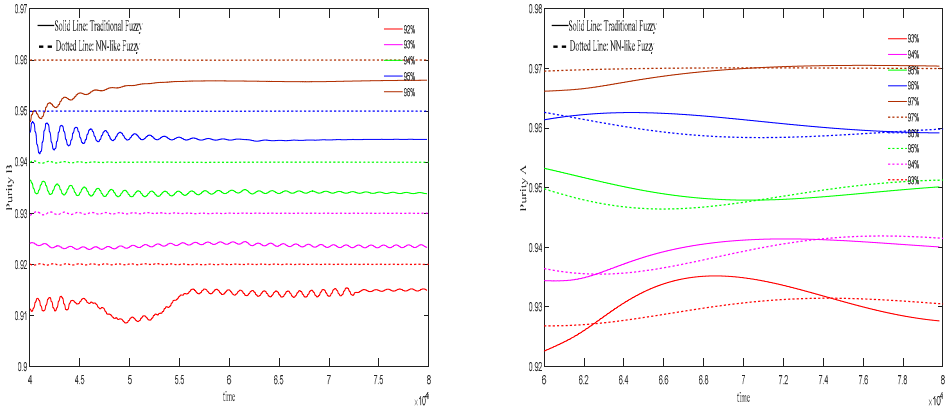

Figure 23. Comparison of two controllers under the disturbance of feed port concentration.

$$C_f = 4.5 \rightarrow 5.2$$

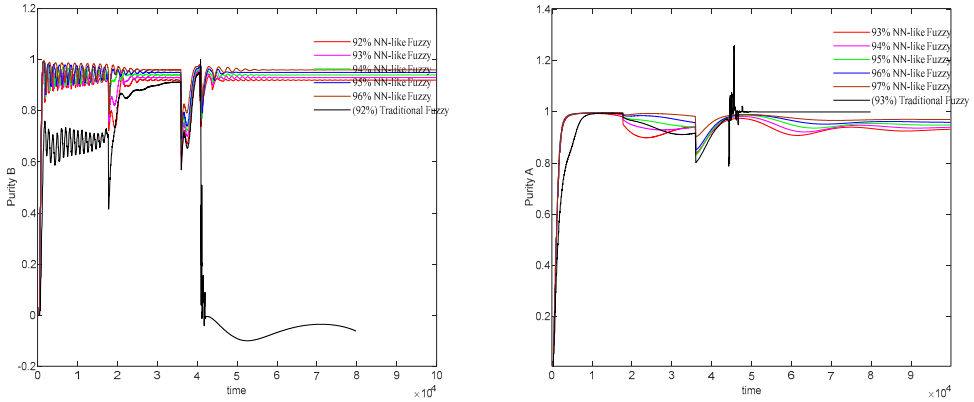

Figure 24. Comparison of two controllers under the disturbance of switch time.

$$\theta = 178s \rightarrow 182s$$

7. Conclusions

This paper explores the digitalization of the SMB process using the Crank-Nicolson method to generate a dynamic model. The method is proven to be stable and convergent for solving the partial differential equations (PDEs) in the SMB process. The study also includes a sensitivity analysis of the regional flow velocity in the SMB system using computer simulations. By observing the effects of different regional velocities on the purity of the extract and raffinate outlets, the researchers identify the monotone region of purity.

Based on the sensitivity analysis and the principles of dynamics, we design fuzzy control rules and incorporate a dynamic learning adjustment function, known as the NN-like fuzzy controller, into the rules. This controller demonstrates high accuracy in controlling the purity of both outlet streams with minimal steady-state error. It also exhibits strong robustness and adaptability to disturbances caused by system parameters such as adsorbent properties, feed port concentration, and switching time.

Compared to the traditional fuzzy controller, the NN-like fuzzy controller not only eliminates steady-state errors but also showcases more robust and adaptive performance in the face of variations and disturbances in various parameters. As a result, the NN-like fuzzy controller is considered an ideal choice for controlling SMB systems that are highly complex and sensitive to parameter changes.

Author Contributions: Conceptualization, Rey-Chue Hwang. and Chao-fan Xie; methodology, Chao-fan Xie.; software, Chao-fan Xie; validation, Rey-Chue Hwang and Chao-fan Xie.; formal analysis, Rey-Chue Hwang;

resources, Rey-Chue Hwang; data curation, Chao-fan Xie, Hong Zhang; writing—original draft preparation, Chao-fan Xie; writing—review and editing, Rey-Chue Hwang; visualization, Hong Zhang, Chao-fan Xie; supervision, Rey-Chue Hwang; project administration, Rey-Chue Hwang. All authors have read and agreed to the published version of the manuscript.

Funding: "This research received no external funding".

Acknowledgments: This research was partially supported by Natural Science Foundation of Fujian Province of China (number: 2023J011117), by the Fujian Province Education Hall Youth Project (number: JAT220258), by the Fujian Natural Science Foundation Project (number: 2019J01887), by the National Natural Science Foundation of China under Grant 62071123，61601125).

Data Availability Statement: To request the corresponding research paper data for experimental simulation, please submit your application via the following email address: liurangzhu@163.com.

Conflicts of Interest: The authors declare no conflict of interest.

References

1. K. M. Kim, K. W. Han, S. I. Kim, and Y. S. Bae, "Simulated moving bed with a product column for improving the separation performance," *Journal of Industrial and Engineering Chemistry*, Vol. 88, No. 25, pp. 328–338, Aug. 2020. DOI:10.1016/j.jiec.2020.04.032.
2. C. S. Reinaldo, B. A. Gomes, and S. A. Resende, "Optimal performance comparison of the simulated moving bed process variants based on the modulation of the length of zones and the feed concentration," *Journal of Chromatography A*, Vol. 1651, pp. 462280-462280, Aug. 2021. DOI:10.1016/J.CHROMA.2021.462280.
3. R. C. Supelano, A. G. Barreto Jr, A. S. A. Neto, and A. R. Secchi, "One-step optimization strategy in the simulated moving bed process with asynchronous movement of ports: A VariCol case study," *Journal of Chromatography A*, Vol. 1634 , pp. 1672-1718, Dec. 2020. DOI:10.1016/j.chroma.2020.461672.
4. S. Li, D. Wei, J. S. Wang, Z. Yan, and S. Y. Wang, "Predictive control method of simulated moving bed chromatographic separation process based on piecewise affine," *International Journal of Applied Mathematics*, Vol. 50, No. 04, pp. 1–12, Dec. 2020.
5. Methodologies; and Product (FlexSMB-LSRE) Development, FEUP, Porto, Portugal, 2009 (Ph.D. thesis).
6. M. Schulte, J. Strube, "Preparative enantioseparation by simulated moving bed chromatography," *Journal of Chromatography A,* 906 (1–2) (2001) 399–416, chiralseparations. DOI: 10.1016/S0021-9673(00)00956-0.
7. K. U. Klatt, F. Hanisch, and G. Dunnebier, "Mode-based control of a simulated moving bed chromatographic process for the separation of frutose and glucose," *Journal of Process Control*, Vol. 12, No. 2, pp. 203-219, Feb. 2002. DOI: 10.1016/S0959-1524(01)00005-1.
8. A. S. Andrade Neto, A. R. Secchi, M. B. Souza, A. G. Barreto, "Nonlinear model predictive control applied to the separation of praziquantel in simulated moving bed chromatography", *Journal of Chromatography A,* pp. 42-49, 2016. DOI: 10.1016/j.chroma.2016.09.070.
9. I. B. Nogueira，M. A. Martins，A. E. Rodrigues，J. M. Loureiro，A. M. Ribeiro, "Novel Switch Stabilizing Model Predictive Control Strategy Applied in the Control of a Simulated Moving Bed for the Separation of Bi-Naphthol Enantiomers", *Industrial & Engineering Chemistry Research*, pp. 1979-1988, 2020.
10. Ju Weon Lee, AndreasSeidel-Morgenstern, Model Predictive Control of Simulated Moving Bed Chromatography for Binary and Pseudo-binary Separations: Simulation Study, *IFAC-PapersOnLine* ,Vol. 51, No. 18, pp. 530-535, 2018. DOI: 10.1016/j.ifacol.2018.09.370.
11. Yonghui Yang, Xuebo Chen, Na Zhang, "Optimizing control of adsorption separation processes based on the improved moving asymptotes algorithm," *Adsorption Science & Technology*, Vol. 36(9–10) ,pp. 1716–1733, 2018. DOI: 10.1177/0263617418804001.
12. V. Carlos, and V. W. Alain, "Combination of multi-model predictive control and the wave theory for the control of simulated moving bed plants," *Journal of Chemical Engineering Science*, 2011, Vol. 66, No. 4, pp. 632-641. DOI: 10.1016/j.ces.2010.11.022.
13. P. Suvarov, A. Kienle, C. Nobre, G. D Weireld, and A. V. Wouwer, "Cycle to cycle adaptive control of simulated moving bed chromatographic separation processes," *Journal of Process Control*, Vol. 24, No. 2, pp. 357-367, Jan. 2014. DOI: 10.1016/j.jprocont.2013.11.001.
14. R. T. Maruyama, P. Karnal, T. Sainio, and A. Rajendran, "Design of bypass -simulated moving bed chromatography for reduced purity requirements," *Journal of Chemical Engineering Science*, Vol. 205, pp. 401-413, Sep. 2019. DOI: 10.1016/j.ces.2019.05.003.

15. M. Leipnitz, A. Biselli, M. Merfeld, N. Scholl, and A. Jupke, "Model-based selection of the degree of cross-linking of cation exchanger resins for an optimized separation of monosaccharides," *Journal of Chromatography A*, Vol. 1610, No. 11, pp. 460565-460576, Jan. 2020. 2020. DOI: 10.1016/j.chroma. 2019.460565.
16. J. C. Schulze, A. Caspari, C. Offermanns, A. Mhamdi, and A. Mitsos, "Nonlinear model predictive control of ultra-high-purity air separation units using transient wave propagation model ", *Computers & Chemical Engineering*, Vol. 145, pp.107163-1-107163-10, 2021. DOI: 10.1016/j.compchemeng.2020.107163.
17. Woo-Sung Lee and Chang-Ha Lee, "Dynamic modeling and machine learning of commercial-scale simulated moving bed chromatography for application to multi-component normal paraffin separation NSTL", *Separation and Purification Technology*, Vol. 288, No. 120597, pp. 2-17, 2022. DOI: 10.1016/J.SEPPUR.2022.120597.
18. H. Marrocos, I. G. I. Iwakiri, M. A. F. Martins, A. E. Rodrigues, J. M. Loureiro, A. M. Ribeiro, I. B. R. Nogueira, "A long short-term memory based Quasi-Virtual Analyzer for dynamic real-time soft sensing of a Simulated Moving Bed unit ", *Applied Soft Computing*, Vol. 116, No. 1083, pp. 1-18, 2022. DOI: 10.1016/J.ASOC.2021. 108318.
19. O. T. Hoon, K. J. Woo, S. S. Hwan, K. Hosoo, L. Kyungmoo, and L. J. Min, "Automatic control of simulated moving bed process with deep Q-network," J*ournal of Chromatography A,* Vol. 1647, pp. 462073-462073, Oct. 2021. DOI: 10.1016/ J.CHROMA.2021.462073.
20. P.S. Gomes, Advances in Simulated Moving Bed: New Operating Modes; New Design Methodologies and Product (FlexSMB-LSRE) Development, FEUP,Porto, Portugal, 2009 (Ph.D. thesis).
21. Bijan Medi, Kazi Monzure-Khoda, and Mohammad Amanullah, "Experimental implementation of optimal control of an improved single-column chromatographic process for the separation of enantiomers", *Ind. Eng. Chem. Res.*, 54 (25), pp 6527–6539, 2015. DOI: 10.1021/acs.iecr.5b00553.
22. C. F. Xie, H. C. Huang, L. Xu, Y. J. Chen and R. C. Hwang, "Adaptive Fuzzy Controller Design for Simulated Moving Bed System," *Sensors and Materials*, 2020, Vol. 32, No. 9, pp.3073–3082. DOI: 10.18494/SAM.2020.2735.
23. I. B. Nogueira R, A. M. Ribeiro, M. A. F. Martins, A. E. Rodrigues, H. Koivisto, J. M. Loureiro, "Dynamics of a True Moving Bed separation process: Linear model identification and advanced process control," *J Chromatogr A*. 2017 Jun 30;1504:112-123. DOI: 10.1016/j.chroma.2017.04.060.
24. S. Mun and N. H. L. Wang, "Improvement of the performances of a tandem simulated moving bed chromatography by controlling the yield level of a key product of the first simulated moving bed unit," *Journal of Chromatography A*, 2017,vol. 1488, pp. 104–112. DOI: 10.1016/j.chroma.2016.12.052.
25. Zhen Yan, Jie-Sheng Wang, Shao-Yan Wang, Shou-Jiang Li, Dan Wang, and Wei-Zhen Sun, "Model Predictive Control Method of Simulated Moving Bed Chromatographic Separation Process Based on Subspace System Identification", *Mathematical Problems in Engineering*, Vol. 7, pp.1-24, 2019. DOI: 10.1155/2019/ 2391891.
26. G. Dunnebier，I. Weirich，K. U. Klatt, "Computationally efficient dynamic modelling and simulated moving bed chromatographic processes with linear isotherms", *Chemical Engineering Science*, Vol. 53, No. 14, pp. 2537-2546, 1998. DOI: 10.1016/ S0009-2509(98)00076-1.
27. M. T. Liang, R. C. Liang, L. R. Huang, P. H. Hsu, Y. H. Wu, and H. E. *Yen,* "Separation of Sesamin and Sesamolin by a Supercritical Fluid-Simulated Moving Bed," *American Journal of Analytical Chemistry*,2012, Vol.3, No.12A, pp.931-938. DOI:10.4236/ajac.2012.312A123.
28. J.-S.R. Jang, "ANFIS: adaptive-network-based fuzzy inference system", *IEEE Transactions on Systems, Man, and Cybernetics*, 1993, Vol. 23, Issue 3, pp. 665-685. DOI: 10.1109/21.256541.
29. P. Y. Tsai, H. C. Huang, Y. J. Chen, S. J. Chuang, R. C. Hwang, "The model reference control by adaptive PID-like fuzzy-neural controller", 2005 IEEE International Conference on Systems, Man and Cybernetics, pp. 239-244, DOI: 10.1109/ICSMC.2005.1571152.